Molecular interpretation of the oscillations of the fusion excitation function for the $\alpha + {}^{40}Ca$ system

F. Michel
Faculté des Sciences, Université de l'Etat, B-7000 Mons, Belgium

G. Reidemeister
Physique Nucléaire Théorique, CP229, Université Libre de Bruxelles, B-1050 Bruxelles, Belgium

S. Ohkubo
Department of Applied Science, Kochi Women's University, Kochi 780, Japan
(Received 27 December 1985)

The oscillations observed in the experimental $\alpha + {}^{40}Ca$ fusion excitation function between $E_\alpha = 10$ and 27 MeV are described within the frame of the optical model. Use is made of an existing optical potential giving a precise description of the elastic scattering data for $E_\alpha > 24$ MeV on a broad angular range, which is extrapolated to lower incident energies. A correct description of elastic scattering experimental excitation functions between $E_\alpha = 12$ and 18 MeV, as well as of the fusion excitation function, is achieved by using different imaginary geometries for both processes. The oscillations appearing in the calculated fusion excitation function are due to maxima in the even-l transmission coefficients, for l ranging from 6 to 12; these maxima correspond to shape resonances in the underlying potential, which are associated with states belonging to an excited positive parity band with $N = 14$ in the $\alpha + {}^{40}Ca$ system. The same potential predicts an $N = 12$ positive parity band of states whose energies are in good agreement with the ${}^{44}Ti$ experimental ground state band. It is shown that the correct reproduction of the spacing between the fusion oscillations achieved here results from the use of a deep real potential, which automatically yields a decoupling between positive and negative parity bands.

I. INTRODUCTION

Fusion excitation functions have been measured for a wide range of heavy-ion systems (for a recent survey of the available experimental data, see, e.g., Ref. 1). The average behavior of the data can be satisfactorily explained within the frame of various semiclassical or potential models.[2] Of particular interest[3] has been the observation, for a limited number of light systems, of a broad oscillatory structure in the measured fusion cross sections as a function of the incident energy; in particular oscillations, a few MeV's wide, have been seen for the ${}^{12}C + {}^{12}C$ (Ref. 4), ${}^{14}C + {}^{14}C$ (Ref. 5), ${}^{12}C + {}^{16}O$ (Refs. 6 and 7), ${}^{14}C + {}^{16}O$ (Ref. 8), and ${}^{16}O + {}^{16}O$ (Ref. 9) systems, as well as for systems composed of ${}^{12}C$ or ${}^{16}O$ plus various 4n *sd*-shell nuclei.[10] The finer structure possibly superimposed on this gross structure[7] is not considered here.

For symmetric systems the observed structures have been interpreted as being due to successive shape resonances whose angular momenta increase in steps of two units;[11] this spacing is peculiar to these systems since even waves only are active in this case. For nonsymmetric systems like ${}^{12}C + {}^{16}O$ it has been repeatedly pointed out that the shallow potentials currently in use for describing the elastic scattering data predict an odd-even alternation of the successive shape resonances, resulting in a smaller spacing and a smoother behavior for the predicted oscillations, in contradiction to experiment. It has been suggested[12] that the parity dependence of the optical potential thought to be present for these systems could result in a staggering of the odd and even partial waves, bringing the spacing of the calculated structures in agreement with the data.

In this paper we investigate another nonsymmetric system where broad oscillations were detected some time ago,[13] i.e., $\alpha + {}^{40}Ca$. Fusion cross sections were measured at the time between $E_\alpha = 10$ and 27 MeV in connection with the anomalous large-angle scattering (ALAS) observed in the elastic channel (see, e.g., Ref. 14 and references therein); the large difference observed between the $\alpha + {}^{40}Ca$ and the neighboring system $\alpha + {}^{44}Ca$ fusion cross sections was shown[13] to support the optical model interpretation put forward to explain the backward enhancement phenomenon.[14-16] However, the broad oscillatory structure seen in the $\alpha + {}^{40}Ca$ fusion data was not studied in the work of Eberhard *et al.*,[13] and—to our knowledge—it has never been investigated since.

Because of the ALAS puzzle, the $\alpha + {}^{40}Ca$ system has been extensively studied both from an experimental and a theoretical point of view. In particular, the exceptionally low absorption which was shown to be responsible for the phenomenon has allowed a precise determination of the real part of the underlying optical potential down to very small distances, as compared to most neighboring systems where the stronger absorption precludes such an accurate determination. Therefore we feel that the precise knowledge of the interaction potential extracted for that particular system may help to clarify the mechanism underlying the fusion oscillations.

II. ANALYSIS

The extensive optical model analysis performed by Delbar *et al.*[14] of elastic $\alpha+^{40}$Ca data for energies ranging from $E_\alpha=24.1$ to 166.0 MeV resulted in the extraction of a global optical potential whose real and imaginary parts, of squared Woods-Saxon shapes, have energy-independent geometrical parameters. The simplest version of this potential ("potential A") can be written as

$$V(r)=V_C(r)-U_0 f^2(r,R,a)-iW_0 f^2(r,R_W,a_W)\ , \tag{2.1}$$

with

$$f(r,R,a)=\{1+\exp[(r-R)/a]\}^{-1}\ , \tag{2.2}$$

and where $V_C(r)$ is the Coulomb potential due to a uniformly charged sphere of radius $1.3A^{1/3}$ fm$=4.446$ fm. The geometrical parameters have the values

$$\begin{aligned} R&=4.685 \text{ fm}\ ,\\ a&=1.290 \text{ fm}\ ,\\ R_W&=6.000 \text{ fm}\ ,\\ a_W&=1.000 \text{ fm}\ . \end{aligned} \tag{2.3}$$

The real well depth varies linearly with energy according to

$$U_0=198.6(1-0.00168E_\alpha) \text{ MeV}\ ; \tag{2.4}$$

the energy behavior of the imaginary strength was shown to be adequately represented by a linear prescription between 24 and 62 MeV:

$$W_0(E_\alpha)=(2.99+0.288E_\alpha) \text{ MeV}\ , \tag{2.5}$$

while some saturation is needed at higher energy.

The simple potential defined by Eqs. (2.1)–(2.5) was shown to give a remarkable description of the complicated evolution of the data on the broad investigated energy and angular ranges, including the backward enhancement seen at low energy and its progressive disappearance above about 50 MeV. Moreover, this potential is unique since it fits high energy data exhibiting rainbow scattering and satisfying the criteria of Goldberg and Smith.[17]

Extrapolation of that potential at lower energies is complicated by the appearance of Ericson fluctuations[18–20] which prevent a detailed comparison of calculated cross sections with existing high resolution data. Even a comparison with energy-averaged angular distributions like those supplied by Bisson *et al.*[20] is hindered by the presence below 18 MeV of a sizeable compound elastic contribution which culminates at about $E_\alpha=10$ MeV. Taking this contribution into account would require a Hauser-Feshbach calculation, which was not attempted here. Therefore we restricted the study of the low-energy properties of the Delbar *et al.* potential to a comparison of its predictions with the excitation functions of Robinson *et al.*[18] which span the 12–18 MeV energy range.

Two minor modifications were imposed to the energy dependences [(2.4) and (2.5)] of the original potential. First, the linear energy dependence of the imaginary depth [cf. Eq. (2.5)] was multiplied by the cutoff factor

$$F(E_\alpha)=\{1-\exp[-(E_\alpha-E_\alpha^{(0)})/\Delta]\}\ ,$$

where $E_\alpha^{(0)}\simeq 3.7$ MeV is the threshold energy and Δ was fixed rather arbitrarily at the value of 5 MeV. This modification guarantees that absorption cancels at the threshold; at the lowest energy investigated here for elastic scattering (i.e., $E_\alpha=12$ MeV), it causes a departure of some 20% from the original parametrization. Second, we fixed the real well depth to the value $U_0=180$ MeV (the corresponding real potential will be referred to as D180 in the following), which is somewhat lower than that obtained from Eq. (2.4) for the energy range considered here. It is to be noted in this respect that prescription (2.4), whose slope parameter was essentially determined by the high energy data, does not prove entirely satisfactory in the 20–30 MeV laboratory energy range, since it predicts volume integrals per nucleon pair $J_V/4A$ of some 370 MeV fm^3, whereas model-independent analyses of the same data[21,22] lead to volume integrals of about 350 MeV fm^3; our choice $U_0=180$ MeV corresponds to $J_V/4A=350$ MeV fm^3. Also there exist theoretical indications[23–25] that some saturation of the real α-nucleus potential should appear at low energy. An independent empirical indication of the need for some saturation with respect to prescription (2.4) comes from spectroscopic considerations concerning the energy location of the members of the ground state band of ^{44}Ti with respect to the threshold (see below).

A comparison of the predictions of the potential thus defined with Robinson *et al.* low energy excitation functions[18] is presented in Fig. 1; it can be seen that the overall energy trends of the data are very satisfactorily reproduced by the calculation. At c.m. angles $\theta_{\text{c.m.}}=148.9°$ and 176.1°, the calculated cross section is somewhat too large, which could indicate some underestimation of the absorptive strength. The only serious discrepancy appears at 158.1°, where the calculated cross section displays a broad minimum around $E_\alpha\simeq 12$ MeV whereas experiment indicates none; however, examination of the results of Bisson *et al.*[20] indicates that the Hauser-Feshbach contribution at this angle is quite sufficient to fill the predicted minimum. In contrast, the other minimum predicted by our calculation at $\theta_{\text{c.m.}}=139.7°$ for $E_\alpha\simeq 15$ MeV is not hidden by the compound nucleus contribution, in agreement with calculations of Bisson *et al.* Although not presented here, the predictions of our potential have also been compared with the lower energy excitation functions of John *et al.*[19] between $E_\alpha=5.0$ and 12.5 MeV. Good agreement is obtained with the average experimental cross sections; the largest discrepancy consists in an underestimation of the experimental data for $\theta_{\text{c.m.}}>90°$, which is maximum for energies where the compound elastic cross section is the largest.[20]

As can be seen in Fig. 2, the total reaction cross section

$$\sigma_R=\pi\lambda^2\sum_l(2l+1)(1-|S_l|^2)$$

calculated with our potential does not show any conspicuous structure, and it is larger at all energies than the fusion cross section of Eberhard *et al.*[13] (It should be noted that the data of Ref. 13 are not corrected for the en-

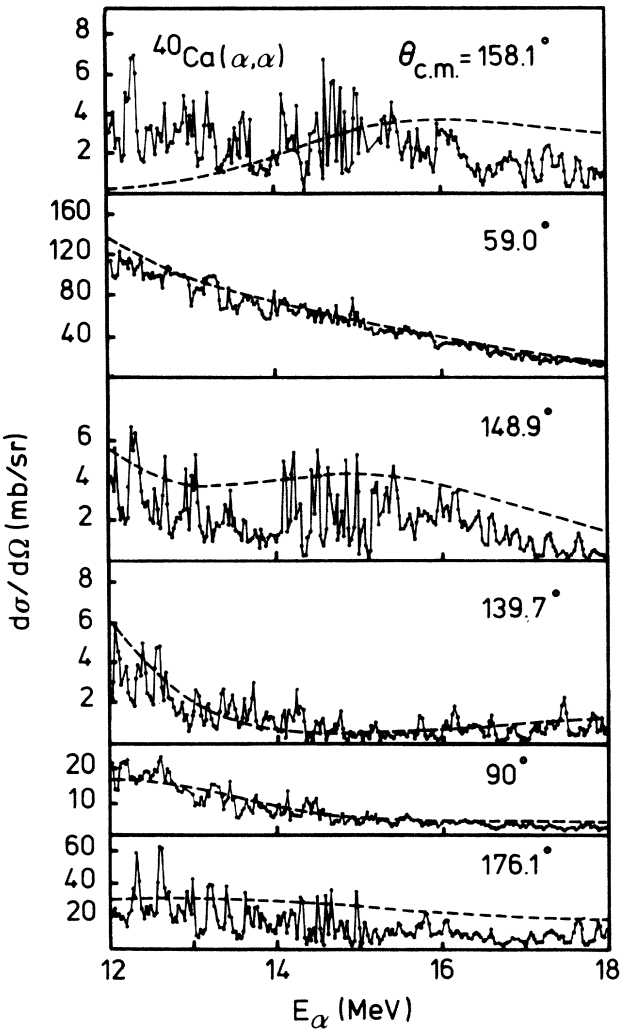

FIG. 1. Comparison of the elastic scattering excitation function for the $\alpha + ^{40}$Ca system, calculated with the D180 potential (dashed line), with the experimental data of Ref. 18 (points).

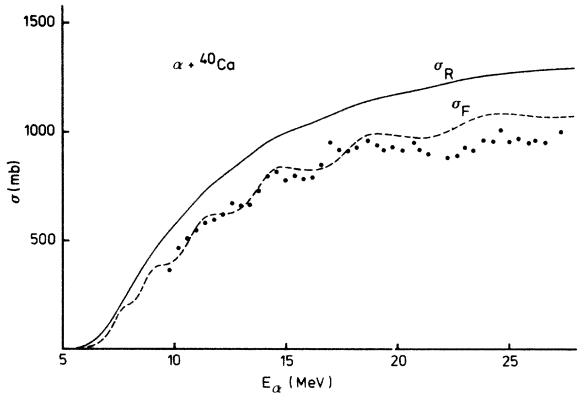

FIG. 2. Reaction (σ_R, solid line) and fusion (σ_F, dashed line) excitation functions, calculated with the D180 potential, together with the experimental data of Eberhard *et al.* (Ref. 13) (points). The experimental errors, which are of the order of 5%, are not shown for clarity.

ergy loss in the target, which is stated to be about 850 keV at $E_\alpha = 10$ MeV. Taking this correction into account would bring the calculated reaction cross section in better agreement with the fusion data at the lowest energies; however, it was not taken into account here since this correction is rather small and energy dependent.) Although slightly larger, our calculated reaction cross section is in good agreement with that extracted by Bisson *et al.*[20] from their optical model plus compound nucleus analysis.

For light heavy-ion systems like $^{12}C + ^{12}C$, it has been pointed out[4] that the oscillations observed in the fusion data could be described qualitatively by empirically reducing the absorption needed for the optical model description of the elastic scattering data. For heavier systems such as $^{16}O + ^{208}Pb$, an empirical reduction of the range of the imaginary potential which correctly describes the reaction excitation function and elastic scattering has also been shown[26] to successfully reproduce the fusion excitation function. More recently the success of this type of prescription has been invoked[27] to support the neglect of the surface part of the imaginary potential in the calculation of proton and alpha-particle fusion cross sections. This recipe has been thoroughly used in the systematic study of Hatogai *et al.*,[28] who were able to consistently reproduce the experimental fusion and elastic scattering data for heavy-ion systems ranging from $^{12}C + ^{12}C$ to $^{40}Ca + ^{40}Ca$, using a common real potential but different imaginary geometries for the two processes. While the imaginary potential W_S they use for fusion calculations is short ranged, an additional longer range potential W_L is used for calculating elastic scattering cross sections; the latter is interpreted as being responsible for the direct transitions taking place preferentially in the peripheral region and depleting the elastic channel. The same idea that the imaginary potential responsible for fusion is substantially shorter ranged than that accounting for elastic scattering and reaction data also underlies several other potential models of fusion such as the boundary condition model of Afanas'ev and Shilov[29] or the distorted wave calculation recently developed by Udagawa and Tamura,[30] and is in line with the concept of a critical distance for fusion.[31] The neglect of the long range part of the imaginary potential in the fusion calculation is more difficult to justify, as it would seem that some depopulation of the incident flux due to the surface transitions caused by W_L must occur before fusion can take place. One can argue that if peripheral direct transitions indeed depopulate the elastic channel, they do not necessarily imply an important loss of flux for the fusion channel[28] since they can represent the first steps towards a fusion event.[32] Still it is clear that, however successful it has proved for reproducing experimental fusion data, the somewhat *ad hoc* prescription of calculating the fusion cross section as a reaction cross section using only the fusion part W_S of the imaginary potential still awaits further justification. We note that for the $^{12}C + ^{12}C$ and $^{16}O + ^{16}O$ systems, the fusion cross sections calculated by Hatogai *et al.*[28] have an oscillatory structure similar to that observed experimentally, which is due to potential resonances in the optical potential with the short range imaginary part W_S; in

contrast the cross section they calculate for the $^{12}C + ^{16}O$ system is smooth, contrary to experiment, probably because of the overlapping of the odd- and even-l resonant contributions mentioned in the Introduction.

Proceeding along these lines, we repeated the $\alpha + ^{40}Ca$ reaction cross section calculation after reducing the imaginary potential radius; good agreement with the absolute value of the experimental fusion cross section is obtained for an imaginary radius $R_W = 4$ fm [instead of the value of 6 fm needed for reproducing the elastic scattering data; cf. Eq. (2.3)]. More important, oscillations with correct widths, spacing, and peak-to-valley ratios automatically emerge from the calculations, as can be seen from inspection of Fig. 2. The origin of these oscillations is most clearly demonstrated by decomposing the calculated fusion cross section σ_F into its various partial cross sections σ_F^l; the result of this decomposition is presented in Fig. 3. It is seen that partial waves with $l = 2$, 4, 6, 8, 10, and 12 are responsible for the six structures appearing in the calculation. In contrast, the odd-l partial cross sections display a much smoother energy behavior. A confirmation of the absence of the odd partial waves in the building up of the oscillations is provided by the selective summation σ_F^{odd} of all the odd-l partial fusion cross sections: The resulting curve, which also appears in Fig. 3, is completely smooth, except above about 20 MeV, where one can discern a slight undulation due to the $l = 11$ partial wave.

The sensitivity of the calculated structures on the real potential well depth was investigated by repeating the above calculations with values of U_0 ranging from 170 to 200 MeV in 5 MeV steps (the corresponding potentials will be referred to as D170 to D200; their volume integrals $J_V/4A$ range from 331 to 389 MeV fm^3); the results of that numerical experiment are displayed in Fig. 4(a). As expected, the calculated oscillations shift as a whole when U_0 is varied. The good agreement with experiment obtained for $U_0 = 180$ MeV is seen to deteriorate rapidly when U_0 departs from that value. On the other hand, shifting the calculated oscillatory structure by one full "wavelength," so that agreement with experiment is obtained with values of the angular momentum differing by two units from those given above, would require a change of the real well depth totally incompatible with a smooth extrapolation of the original potential of Delbar *et al.* (and it would ruin the good agreement obtained for the elastic scattering data). It can therefore be safely concluded that the spins assigned above to the calculated structures are unambiguous.

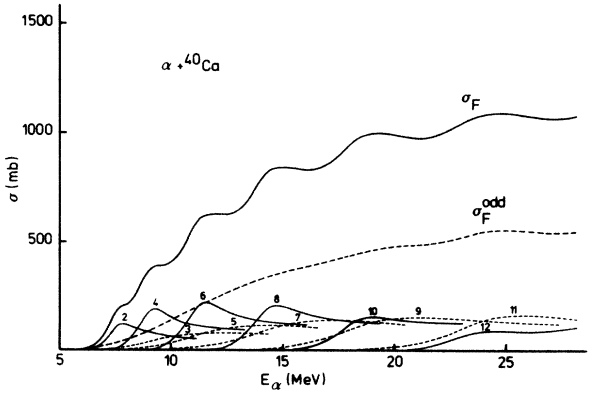

FIG. 3. Decomposition of the fusion cross section σ_F calculated with the D180 potential (heavy solid line) into partial fusion cross section contributions σ_F^l (even l: thin solid lines; odd l: thin dashed lines); also shown is the result σ_F^{odd} of the selective summation of all odd-l partial cross sections (heavy dashed line).

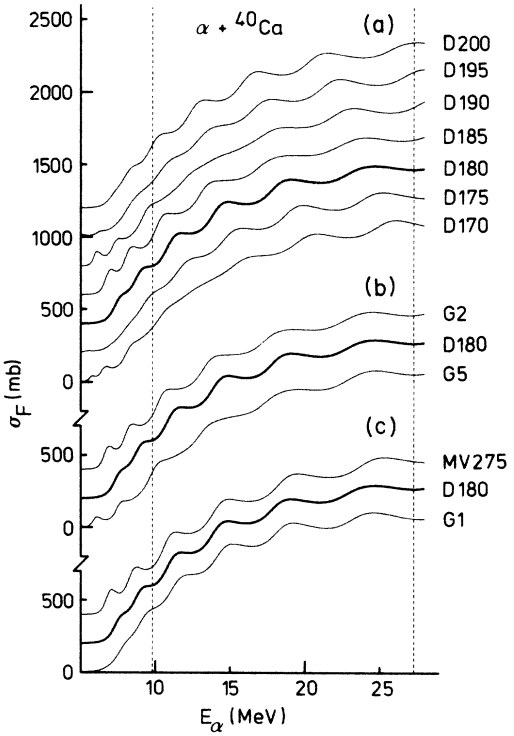

FIG. 4. (a) Dependence of the calculated fusion cross section on the potential depth U_0 (U_0 ranges from 170 to 200 MeV in 5 MeV steps). (b) Calculated fusion excitation function for various potentials belonging to the $J_V/4A \simeq 350$ MeV fm^3 potential family (see the text). (c) Calculated fusion excitation function for potentials belonging to adjacent families (see the text). In each part of the figure, the heavy line represents the fusion excitation function calculated with the D180 potential (cf. Figs. 2 and 3), and the curves have been shifted vertically from the lowest one by multiples of 200 mb. The vertical dotted lines delimit the energy range spanned by the fusion data of Eberhard *et al.* (Ref. 13).

A related point of interest is to examine to what extent the results obtained here are peculiar to the potential investigated. For that purpose we calculated the fusion cross section using two real potentials obtained independently by Gubler *et al.*[22] from an extensive optical model analysis of their $^{40}Ca(\alpha,\alpha)$ data. Both belong to the same potential family as the potential of Delbar *et al.*, i.e., to the unique family fitting the high energy data. These potentials have a generalized Woods-Saxon shape: one is their potential No. 2 (which we will denote as G2) extracted at 31 MeV incident energy, the other is a Woods-Saxon

raised to the fifth power (denoted here as G5) obtained at 26.1 MeV (all the WS[5] low energy potentials given in Table 3 of Ref. 22 give essentially similar results). Potentials G2 and G5 have volume integrals of 359 MeV fm^3 and 351 MeV fm^3, respectively. To simplify matters the calculations were carried out with the same imaginary potential as above; the resulting fusion excitation functions are presented in Fig. 4(b). From that calculation we can conclude that—provided use is made of a real potential giving a precise description of the low energy elastic scattering data—the properties of the structures appearing in the calculated fusion excitation function (and in particular their spins) do not depend sensitively on fine details of the potential as, e.g., its precise form factor.

Finally, we calculated the fusion excitation function with real potentials belonging to different potential families, to investigate whether the fusion data can discriminate potentials which are equivalent with respect to low energy elastic scattering; the calculations were again carried out with the same imaginary part as before, although it might have been preferable to adjust the imaginary strength in this case. The results reported in Fig. 4(c) were obtained with potential No. 1 of Gubler *et al.*[22] (denoted here as G1) extracted at 31 MeV (which belongs to the shallower potential family, $J_V/4A = 279$ MeV fm^3), and with the potential derived at 29 MeV by Michel and Vanderpoorten[15] [the depth of the latter had to be slightly readjusted from the original value of 287.9 MeV to 275 MeV in order to bring the calculations in precise agreement with the D180 results; this potential (MV275) belongs to the deeper potential family, and with the present normalization the value of its volume integral is 418 MeV fm^3]. It is seen that in the energy range investigated here, the three potentials have very similar properties with respect to fusion calculations. Differences appear only at energies where the scattering properties of the various families also become different, i.e., above 40—50 MeV incident energy.

III. DISCUSSION

In the preceding section it was demonstrated that the structures appearing in the calculated fusion excitation function between 10 and 27 MeV incident energies are due to maxima in the even-l transmission coefficients $T_l = 1 - |S_l|^2$ for l ranging from 6 to 12 (the last structure also contains a sizeable $l = 11$ contribution). These maxima correspond to successive shape resonances in the underlying potential. This is confirmed by the calculation of the elastic scattering excitation function at $\theta = 180°$ using our D180 potential with zero absorption: Broad resonance maxima, well separated in energy, appear at the same locations as those observed in the fusion excitation function (see Fig. 5). Introduction of absorption progressively washes out the observed maxima by reducing their peak-to-valley ratios. Most of the structure fades away when use is made of absorptive strengths fitting the average elastic scattering data; the residual structure predicted by the calculation at low energy cannot be seen in the experimental backward excitation function,[18,19] since elastic scattering is dominated by Ericson fluctuations and com-

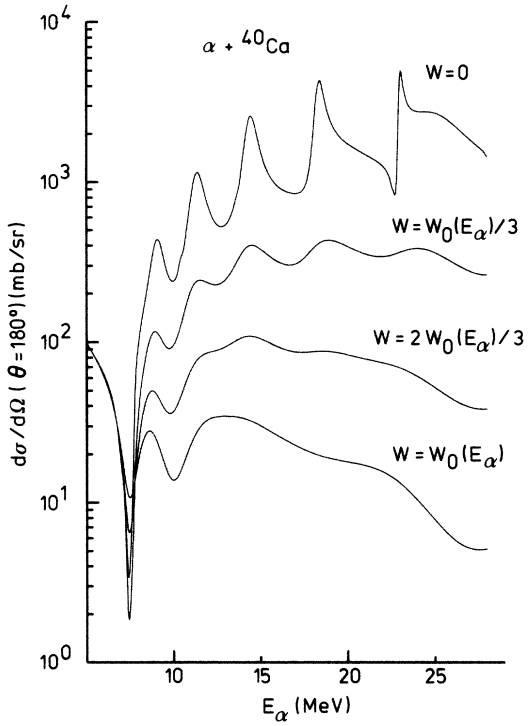

FIG. 5. Backward angle elastic scattering excitation function calculated with the D180 potential for increasing imaginary well depths; $W_0(E_\alpha)$ denotes the absorptive strength used to describe elastic scattering experimental data (cf. Fig. 1).

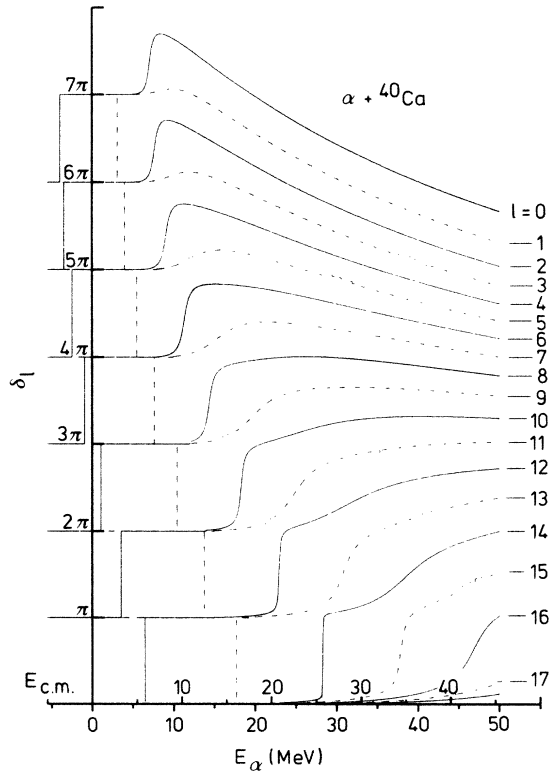

FIG. 6. Absolute phase shifts and bound states calculated with the D180 potential.

pound elastic scattering at these energies.[20]

The nature of the resonances responsible for the fusion structures can be clarified by calculating the absolute phase shifts with the real part of our potential: these are presented in Fig. 6, together with the states bound by the potential down to $E_{\text{c.m.}} = -5$ MeV. Inspection of this figure reveals the existence of three quasirotational bands with principal quantum numbers $N \equiv 2n_r + l$ (where n_r denotes the number of nodes of the radial wave function) equal to 12, 13, and 14; a fourth $N = 15$ band of very broad states is also apparent in Fig. 6. States of the $N = 14$ band with l ranging from 6 to 12 are responsible for the structure appearing in the experimental fusion excitation function (the last structure is influenced by the $l = 11$ state of the $N = 15$ band). Lower energy states of the $N = 15$ band appear to be too broad (the corresponding phase shifts hardly exceed 90°) to be seen in the fusion or elastic scattering excitation functions. On the other hand, states of the $N = 13$ band, located at lower energies, have much too small widths to have any observable influence on these cross sections (in fact these states are responsible for the narrow additional oscillations appearing at the low energy end of the fusion cross section calculated with the shallower D170 potential [cf. Fig. 4(a)], which locates these states higher in energy, and therefore predicts considerably larger widths). The decoupling of the $N = 14$ positive parity band from the $N = 13$ and $N = 15$ negative parity bands thus appears to be an essential feature of our potential for reproducing the structures observed in the fusion excitation function with correct spacings and widths. It is worth noting that this decoupling emerges naturally when use is made of deep potentials whose form factor is not too dissimilar to that of a harmonic oscillator well,[33] and does not require the introduction of a parity dependence in the potential. As to the lower $N = 12$ positive parity band predicted by the potential,[34] it comes in good agreement with the ground state band of ^{44}Ti, although the collapse of the higher members of the band, which is observed experimentally, is not reproduced by the calculation. It is to be noted that the cluster band structure of ^{44}Ti is a matter of controversy and that the interpretation emerging from the present study disagrees with some existing attributions;[35,36] further discussion of the spectroscopic aspects of our potential picture of the $\alpha + {}^{40}$Ca system is deferred to a forthcoming publication.

To close this section we comment on the good agreement obtained with the experimental fusion cross section

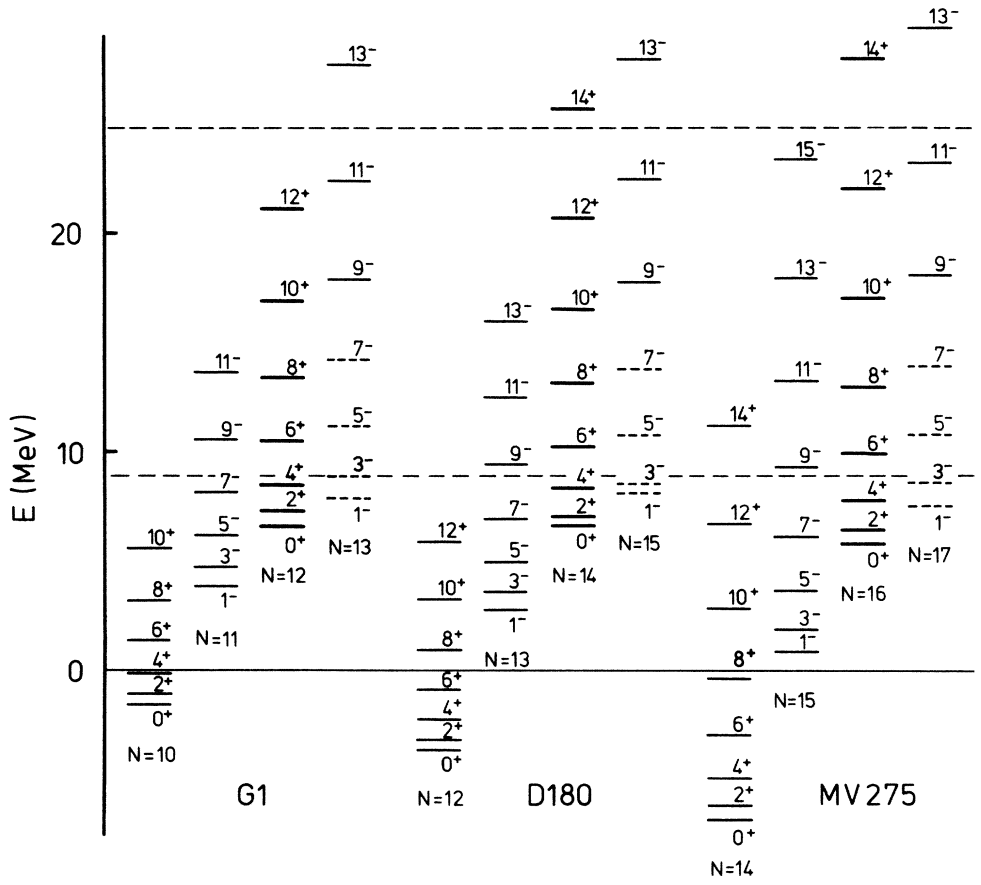

FIG. 7. Comparison of the band structure predicted by potentials belonging to adjacent potential families (see the text). The position of the quasibound states located well below their barrier was calculated using the bound-state approximation, while the position of broader states is defined as the energy where the derivative of the phase shift with respect to energy is the largest (when the phase shift does not pass through $\pi/2$, this position is indicated by an interrupted line). The two dashed lines delimit the energy range spanned by the fusion data of Eberhard *et al.* (Ref. 13).

when use is made of potentials belonging to shallower or deeper families. To this end we have calculated the position of the bound, quasibound, and virtual states predicted by the D180 potential and by the other two potentials (G1 and MV275) used at the end of the preceding section. The results of the calculation appear in Fig. 7; states have been grouped into bands of constant principal quantum number N, and the states responsible for the structure seen in the fusion excitation function are represented with thicker lines. The energy range scanned by the experimental fusion data analyzed here appears also in Fig. 7. It can be seen that the three potentials predict essentially similar results within this range. The only important difference lies in the nature of the bands supporting the various states. For example, the positive parity band responsible for the structure in the fusion cross section, which is an $N=14$ band when calculated with the D180 potential, becomes an $N=12$ or $N=16$ band when calculated with potentials of the shallower or deeper family, respectively. The $J^{\pi}=14^{+}$ state of this band (which lies outside the investigated energy range) is thus missing for the shallower potential, while an additional $J^{\pi}=16^{+}$ state is predicted by the deeper one. In the same way the $N=15$ band, which has small influence on the fusion calculation (except for its $J^{\pi}=11^{-}$ member) becomes an $N=13$ or $N=17$ band, respectively, when calculated with the alternative potentials; in the energy region scanned by experiment, however, the predicted levels have very similar energies. In contrast, the ending of these bands at different angular momenta has a profound influence on the elastic scattering properties of the three potentials: the shallower or deeper potential predicts the onset of the rainbow scattering regime[17] at too low or too high energies, respectively. Finally the two lower bands, which correspond to $N=12$ and $N=13$ when calculated with the D180 potential, lose or gain, respectively, one state with the shallower or deeper potential, respectively; however, since the corresponding states appearing above the threshold are located well below their respective barriers, they have exceedingly small widths and their influence on fusion or elastic scattering is completely negligible.

IV. SUMMARY AND CONCLUSIONS

In this paper we have shown that a natural extrapolation of the potential originally used by Delbar *et al.*[14] to describe α-particle scattering from ^{40}Ca from 24 to 166 MeV provides a good description of the low energy properties of the system as well: We have succeeded in reproducing both the low-energy elastic scattering excitation functions measured by Robinson *et al.*[18] between 12 and 18 MeV at several angles (though comparison with experiment is somewhat complicated by the occurrence of Ericson fluctuations and compound elastic scattering) and the fusion excitation function of Eberhard *et al.*[13] between 10 and 27 MeV, including the broad oscillations showing up throughout that range. This was accomplished by using a common real potential well but different imaginary geometries for the two processes, in the spirit of a recent work of Hatogai *et al.*:[28] The imaginary radius we used for fusion calculations is smaller than that needed for describing the elastic scattering data. This mechanism allows the calculated fusion excitation function to exhibit oscillations whereas the calculated reaction cross section displays a smooth energy behavior. These oscillations have been shown to be due to even-l shape resonances with spins ranging from 6 to 12 (with some admixture of $l=11$ in the last oscillation), and they have been associated with molecular states belonging to an excited positive parity band with $N=14$ in ^{44}Ti. In addition, the same real potential supports another band of positive parity states with $N=12$, whose energies are in good agreement with those of the experimental ground state band of ^{44}Ti. It was checked that the properties of the structures observed in the calculated fusion cross section (and in particular their spins) do not depend critically in the investigated range on the particular potential used—nor on the potential family—provided use is made of a potential giving a good description of the low energy elastic scattering data.

A single real potential thus proves capable of describing in a consistent fashion—and with a minimum number of varying parameters—a wide range of properties of the $\alpha+^{40}$Ca system, extending from negative up to high excitation energies. Although such unified potential descriptions have been known for a long time for nucleon-nucleus systems (see, e.g., Refs. 37 and 38), they have remained scarce for composite particle scattering; in this context, mention should be made of the systematic local potential study recently performed for the $\alpha+^{16}$O system.[39]

As was discussed in the preceding section, the decoupling between positive and negative parity bands, which automatically emerges from a potential description making use of deep real potentials, is a decisive feature for a correct description of the fusion oscillations observed in the data analyzed here. Although the common practice has been to use real potentials of shallow type for describing light heavy-ion elastic scattering, it appears that the local potentials which are equivalent to the resonating group nonlocal potentials are necessarily very deep[40–42] (the depth of the potential recently derived by Wada and Horiuchi[43] for the ^{16}O + ^{16}O system is about 400 MeV). Therefore solution of the ^{12}C + ^{16}O puzzle mentioned in the Introduction could require explicit use of such deep potentials, although the importance of parity dependence effects[12] should not be overlooked, since these are expected to be important for nearly symmetric systems.[44,45]

ACKNOWLEDGMENTS

One of the authors (S.O.) is grateful to Professor R. Ceuleneer for having made possible his stay at the University of Mons. He is also thankful to Professor D. M. Brink for useful discussions on fusion reactions. F.M. and G.R. are very indebted to Professor R. Ceuleneer for his constant interest and for his careful reading of our manuscript. S.O. is grateful to the Institut Interuniversitaire des Sciences Nucléaires for financial support.

[1]P. Fröbrich, Phys. Rep. **116**, 337 (1984).
[2]J. R. Birkelund, L. E. Tubbs, J. R. Huizenga, J. N. De, and D. Sperber, Phys. Rep. **56**, 107 (1979); L. C. Vaz, J. M. Alexander, and G. R. Satchler, *ibid.* **69**, 373 (1981).
[3]U. Mosel, in *Treatise on Heavy Ion Science,* edited by D. A. Bromley (Plenum, New York, 1984), Vol. 2, p. 3.
[4]P. Sperr, T. H. Braid, Y. Eisen, D. G. Kovar, F. W. Prosser, Jr., J. P. Schiffer, S. L. Tabor, and S. Vigdor, Phys. Rev. Lett. **37**, 321 (1976); J. J. Kolata, R. M. Freeman, F. Haas, B. Heusch, and A. Gallmann, Phys. Rev. C **21**, 579 (1980).
[5]R. M. Freeman, C. Beck, F. Haas, B. Heusch, H. Bohn, U. Kaüfl, K. A. Eberhard, H. Puchta, T. Senftleben, and W. Trautmann, Phys. Rev. C **24**, 2390 (1981).
[6]J. J. Kolata, R. M. Freeman, F. Haas, B. Heusch, and A. Gallmann, Phys. Lett. **65B**, 333 (1976); P. Sperr, S. Vigdor, Y. Eisen, W. Henning, D. G. Kovar, T. R. Ophel, and B. Zeidman, Phys. Rev. Lett. **36**, 405 (1976).
[7]A. D. Frawley, N. R. Fletcher, and L. C. Dennis, Phys. Rev. C **25**, 860 (1982).
[8]J. J. Kolata, C. Beck, R. M. Freeman, F. Haas, and B. Heusch, Phys. Rev. C **23**, 1056 (1981).
[9]J. J. Kolata, R. C. Fuller, R. M. Freeman, F. Haas, B. Heusch, and A. Gallmann, Phys. Rev. C **16**, 891 (1977); B. Fernandez, C. Gaarde, J. S. Larsen, S. Pontoppidan, and F. Videbaek, Nucl. Phys. **A306**, 259 (1978).
[10]I. Tserruya, J. Barrette, S. Kubono, P. Braun-Munzinger, M. Gai, and D. C. Uhlhorn, Phys. Rev. C **21**, 1864 (1980); P. A. De Young, J. J. Kolata, R. C. Luhn, R. E. Malmin, and S. N. Tripathi, *ibid.* **25**, 1420 (1982); R. M. Freeman, F. Haas, B. Heusch, and S. M. Lee, *ibid.* **20**, 569 (1979); K. Daneshvar, D. G. Kovar, S. J. Krieger, and K. T. R. Davies, *ibid.* **25**, 1342 (1982); W. J. Jordan, J. V. Maher, and J. C. Peng, Phys. Lett. **87B**, 38 (1979); J. J. Kolata, R. A. Racca, P. A. De Young, E. Aguilera-Reyes, and M. A. Xapsos, Phys. Rev. C **32**, 1080 (1985).
[11]Y. Kondo, D. A. Bromley, and Y. Abe, Phys. Rev. C **22**, 1068 (1980).
[12]N. Poffé, N. Rowley, and R. Lindsay, Nucl. Phys. **A410**, 498 (1983).
[13]K. A. Eberhard, Ch. Appel, R. Bangert, L. Cleemann, J. Eberth, and V. Zobel, Phys. Rev. Lett. **43**, 107 (1979).
[14]Th. Delbar, Gh. Grégoire, G. Paic, R. Ceuleneer, F. Michel, R. Vanderpoorten, A. Budzanowski, H. Dabrowski, L. Freindl, K. Grotowski, S. Micek, R. Planeta, A. Strzalkowski, and K. A. Eberhard, Phys. Rev. C **18**, 1237 (1978).
[15]F. Michel and R. Vanderpoorten, Phys. Rev. C **16**, 142 (1977).
[16]H. P. Gubler, U. Kiebele, H. O. Meyer, G. R. Plattner, and I. Sick, Phys. Lett. **74B**, 202 (1978).
[17]D. A. Goldberg and S. M. Smith, Phys. Rev. Lett. **29**, 500 (1972).
[18]C. P. Robinson, J. P. Aldridge, J. John, and R. H. Davis, Phys. Rev. **171**, 1241 (1968).
[19]J. John, C. P. Robinson, J. P. Aldridge, and R. H. Davis, Phys. Rev. **177**, 1755 (1969).
[20]A. E. Bisson, K. A. Eberhard, and R. H. Davis, Phys. Rev. C **1**, 539 (1970).
[21]F. Michel and R. Vanderpoorten, Phys. Lett. **82B**, 183 (1979).
[22]H. P. Gubler, U. Kiebele, H. O. Meyer, G. R. Plattner, and I. Sick, Nucl. Phys. **A351**, 29 (1981).
[23]T. Fliessbach, Nucl. Phys. **A315**, 109 (1979).
[24]K. Aoki and H. Horiuchi, Prog. Theor. Phys. **68**, 2028 (1982).
[25]C. Mahaux, H. Ngô, and G. R. Satchler, Nucl. Phys. **A449**, 354 (1986).
[26]L. C. Vaz, J. M. Alexander, and E. H. Auerbach, Phys. Rev. C **18**, 820 (1978); H. Delagrange, L. C. Vaz, and J. M. Alexander, *ibid.* **20**, 1731 (1979).
[27]L. C. Vaz and J. M. Alexander, in *Proceedings of the International Conference on Fusion Reactions below the Coulomb Barrier,* edited by S. G. Steadman (Springer, Berlin, 1984), p. 288.
[28]K. Hatogai, M. Ohta, and S. Okai, Prog. Theor. Phys. **68**, 2014 (1982).
[29]G. N. Afanas'ev and V. M. Shilov, Yad. Fiz. **26**, 92 (1977) [Sov. J. Nucl. Phys. **26**, 48 (1977)].
[30]T. Udagawa and T. Tamura, Phys. Rev. C **29**, 1922 (1984); T. Udagawa, S. W. Hong, and T. Tamura, *ibid.* **32**, 1435 (1985).
[31]R. Bass, Phys. Lett. **47B**, 139 (1973); J. Galin, D. Guerreau, M. Lefort, and X. Tarrago, Phys. Rev. C **9**, 1018 (1974); D. Glas and U. Mosel, Nucl. Phys. **A237**, 429 (1975).
[32]S. Okai, M. Ohta, and Y. Oyama, Prog. Theor. Phys. **65**, 763 (1981).
[33]N. Rowley, Phys. Lett. **69B**, 25 (1977).
[34]R. Ceuleneer, F. Michel, and G. Reidemeister, in *Proceedings of the Symposium on Resonances in Heavy Ion Reactions,* edited by K. A. Eberhard (Springer, Berlin, 1982), p. 227.
[35]D. Frekers, R. Santo, and K. Langanke, Nucl. Phys. **A394**, 189 (1983).
[36]H. Horiuchi, Prog. Theor. Phys. **73**, 1172 (1985).
[37]S. Gamba, G. Ricco, and G. Rottigni, Nucl. Phys. **A213**, 383 (1973).
[38]M. M. Giannini and G. Ricco, Ann. Phys. (N.Y.) **102**, 458 (1976).
[39]F. Michel, J. Albinski, P. Belery, Th. Delbar, Gh. Grégoire, B. Tasiaux, and G. Reidemeister, Phys. Rev. C **28**, 1904 (1983).
[40]H. Friedrich, Phys. Rep. **74**, 209 (1981).
[41]D. Wintgen, H. Friedrich, and K. Langanke, Nucl. Phys. **A408**, 239 (1983).
[42]K. Aoki and H. Horiuchi, Prog. Theor. Phys. **69**, 1154 (1983).
[43]T. Wada and H. Horiuchi, in contributed papers, Proceedings of the 4th International Conference on Clustering Aspects of Nuclear Structure and Nuclear Reactions, Chester, U.K., 1984, edited by J. S. Lilley and M. A. Nagarajan (unpublished), p. 41.
[44]M. Le Mere, D. J. Stubeda, H. Horiuchi, and Y. C. Tang, Nucl. Phys. **A320**, 449 (1979).
[45]K. Aoki and H. Horiuchi, Prog. Theor. Phys. **69**, 857 (1983).